ACS Macro Letters

Letter

pubs.acs.org/macroletters

Energy Conversion in Polyelectrolyte Hydrogels

Aykut Erbas[†,‡] and Monica Olvera de la Cruz*[,†,‡]

[†]Department of Materials Science and Engineering, Northwestern University, Evanston, Illinois 60208, United States

[‡]Departments of Chemistry, Chemical and Biological Engineering, and Physics and Astronomy, Northwestern University, Evanston, Illinois 60208, United States

ABSTRACT: Using extensive molecular dynamics simulations of polyelectrolyte hydrogels we demonstrate that, on deformation, these hydrogels adjust their deformed state predominantly by altering electrostatic interactions between their charged groups rather than excluded-volume and bond energies. On deformation, due to the hydrogel's inherent tendency to preserve electroneutrality in its interior, the translational entropy of counterions decreases and the total electrostatic energy becomes more attractive. This result is valid for a wide range of compression ratios and Bjerrum lengths. The change in the electrostatic energy is more marked in highly swollen gels at low ionic strengths. At high Bjerrum lengths, where most of the counterions are condensed on hydrogel chains and the gel resembles a neutral system, the electrostatic-energy change with deformation is weaker.

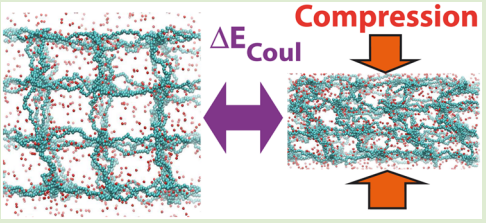

Converting energy between different forms (from mechanical to chemical energy, for example) and storing it safely for future use has been an active field of research in nanotechnology in response to a growing need for sustainable-energy resources. Charged polymeric structures have attracted considerable attention in this field due to their low cost, mechanical flexibility, transparency, and stimuli-responsive properties, which are absent in their conventional solid-state counterparts. Hydrogels that are highly swollen networks of charged polymers have proven effective in various applications, such as mechano-electric energy converters,[1−4] energy storage,[5,6] and even biomimetic structures.[7−9] While the elasticity of hydrogels' constituent chains gives them polymeric properties, their charged or ionizable groups bring additional electrostatic features, such as pH- and electro-responsive characteristics.[10,11] The balance between these inherent electrostatic and elastic properties of hydrogels allows them to adjust their internal electrostatic interactions reversibly upon application of external electromagnetic fields or mechanical deformations. This makes them ideal candidates for energy converters and actuators.

The high-swelling capacity of a polyelectrolyte (PE) hydrogel is due to a balance between the counterion-induced osmotic pressure and the elastic energy of hydrogel chains (i.e., Donnan equilibrium).[12,13] If the hydrogel structure is compressed by an external force, the solvent content in the gel is squeezed out, but the ionized counterions remain in the hydrogel to maintain the electroneutrality inside the hydrogel. If the gel volume is decreased on compression, the deformation leads to an increase in the monomeric concentration. Concurrently, trapped counterions decrease their translational free energy. The electroneutrality condition, in combination with the decrease of intermonomer distance, forces the hydrogel to rebalance its energetic components by adjusting the chain conformations or repositioning its charged groups.

Recently, elegant computational studies have shed light on the equilibrium properties of stress-free hydrogels using molecular dynamics (MD)[14,15] and Monte Carlo (MC)[16−18] simulations. However, gels are deformed and not stress-free in most practical situations. To our best knowledge, there have been no molecular-level studies on the relationship between the electrostatic energy and deformation of PE hydrogels, yet a molecular-level understanding of the electrostatic effects is essential to the development of continuum deformation models, precise theoretical approaches, and advanced PE gel applications.

Here, we investigate the relation between deformation and energetic changes in PE hydrogels by means of MD simulations. We have designed a double gel system in which two semi-infinite hydrogel slabs are separated by a large polymer-free region, to which counterions can escape, as shown in Figure 1. Note that this semiperiodic design does not a priori force counterions to stay in the gel interior upon deformation. We demonstrate that when a PE gel is deformed, the most notable change in the overall energetic balance takes place in the electrostatic energy components rather than in the excluded volume and bond energies. On deformation, the charged backbone groups and counterions arrange themselves so as to minimize the total electrostatic energy and form ionic structures. This is a direct consequence of the electroneutrality condition inside the gel: though counterions gain more entropy outside of the gel, their energetic penalty for leaving the gel is higher. Counterions thus remain in the gel even under very strong compression, and this results in significant alteration of the electrostatic energy.

Received: June 2, 2015
Accepted: July 28, 2015
Published: August 3, 2015

DOI: 10.1021/acsmacrolett.5b00363
ACS Macro Lett. 2015, 4, 857−861

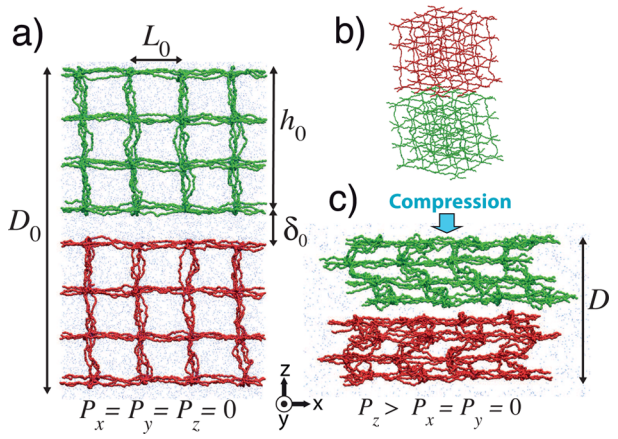

Figure 1. Illustration of compression simulations of a double hydrogel system of identical gels with a charge fraction $f = 0.5$ and polymerization degree $N = 128$. Counterions are rendered as dots. (a) Underformed hydrogel slabs separated initially by a gap of thickness δ_0, (b) 3D view of the hydrogels, and (c) uniaxially compressed gels. Note that the dangling ends at the edges are bonded to those in the adjacent periodic gel. In the actual simulations, $\delta_0 \approx h_0$. All snapshots are obtained via VMD.

METHODS

Various double-hydrogel systems composed of two identical slabs, as shown in Figure 1, are simulated with explicit counterions in implicit good solvent. Each hydrogel slab is constructed as a defect-free cubic polymer lattice. The lattice junction points (cross-links) are permanent. The flexible polymer segments connecting two cross-links of the hydrogel network are modeled using coarse-grained Kremer-Grest (KG) bead−spring model.[19,20] In this model, excluded volume interactions are modeled via a repulsive Lennard-Jones (LJ) potential, whereas bond interactions are modeled with a nonlinear FENE potential. The number of monomers per linear-polymer segment are taken to be $N = 32$ and 128 to obtain various volume fractions $\phi \approx Nb^3/L_0^3$, where L_0 is the distance between two cross-links, as depicted in Figure 1, and b is the size of a LJ monomer. The chemical details of the chains are described by a charge fraction factor f: a prescribed fraction of chain monomers are assigned $q = +1e$ charges. For each positive charge on the backbone, one monovalent charge is added to the simulation box at a random position to model ionized counterions. Hence, the overall system is electro-neutral. The short-range Coulombic interactions between two charged monomers separated by a distance r are calculated via

$$U_C(r) = -\epsilon\frac{l_B}{r} \text{ for r} < r_e \tag{1}$$

where the energy scale is denoted by $\epsilon = 1k_BT$, where k_B is the Boltzmann constant and T is temperature. The strength of electrostatic interactions is characterized by the Bjerrum length $l_B = e^2/4\pi\varepsilon_0\varepsilon\epsilon$, where ε_0 is the vacuum permittivity and ε is the relative dielectric constant of the medium. The Bjerrum length quantifies the length scale, above which the strength of Coulombic energies are less than the thermal energy k_BT. The electrostatic cutoff distance is $r_e = 6b$, above which longer-range electrostatic interactions are calculated via Particle−Particle-Particle Mesh (PPPM) Ewald solver.[21] The strength of the electrostatic interactions in simulations is adjusted by tuning the dielectric constant to obtain $l_B \simeq 1b, 4b, 8b$. As an example, for a hydrogel composed of flexible polymers, each effective monomer of size b is of 2−3 chemical units, hence, $l_B \simeq 1b \approx 7$ Å corresponds to a hydrogel dissolved in water.

In the simulations, the initial vertical box height (i.e., $\hat{z}$ component) is set to $D_0 \approx 12L_0 \approx 4h_0$, where h_0 is the height of a slab (Figure 1). Initially, two gels slabs are separated by a polymer-free gap of thickness $\delta_0 \approx h_0$. While the slabs shown in Figure 1 are finite in the $\hat{z}$-direction, the hydrogel network is periodic in the lateral directions. For the simulation box itself, periodic boundary conditions are introduced in all directions. All MD simulations are run using the Lammps MD package[22] at constant pressure P, particle number N_m, and temperature T. The temperature is set to $T = 1.0\epsilon/k_B$ with the Noose-Hover thermostat. To obtain a stress-free state at D_0, the pressure is set to $P = P_z = P_y = P_z = 0 \pm \delta P$ using anisotropic pressure coupling scheme, where the error tolerance $\delta P \approx 10^{-5} - 10^{-6}k_BT/b^3$ for $N = 32$ and 128 hydrogels, respectively. At $P = 0$, both hydrogel slabs are isotropically swollen.

Simulations of strain-controlled gel deformations: The vertical height of the simulation box, D_0, is brought to a prescribed height $D < D_0$ and equilibrated before the data production runs. To mimic a uniaxial deformation scheme in production runs, the lateral (i.e., $\hat{x}$ and $\hat{y}$) components of barostat are set to $P_x = P_y = 0$ in a coupled fashion, whereas the box height is fixed in the vertical direction. The pressure that is necessary to keep the box height at D is recorded as P_z. In all of the deformation simulations, $P_z \gg P_x \approx P_y \approx 0.0$. Unless noted otherwise, all results presented in this paper are averaged over time. Error bars are not shown if they are smaller than the size of the corresponding data point.

Undeformed gels: When a PE-gel precursor is dissolved in a solvent with weak electrostatic strength, such as water, ionizable backbone groups release their counterions. Due to the electroneutrality condition in the gel, most counterions reside inside the gel and induce an outward osmotic pressure. This osmotic pressure can be expressed by $\Pi_{ci} \approx k_BTNf/L_0^3$ for a dilute system with no electrostatic correlations.[14,23] The elastic energy density of the stretched network chains $\Pi_{el} \approx k_BT(L_0/N^\nu b)^2/L_0^3$, where $\nu \approx 3/5$ is the scaling exponent for good solvent, opposes the counterion-osmotic pressure.[24] From the balance of the two pressures, $\Pi_{ci} \approx \Pi_{el}$, an equilibrium swelling ratio can be defined as

$$\lambda_0 \equiv \frac{L_0}{R_{dry}} = N^{1/2}f^{1-\nu} \tag{2}$$

where the size of a free N-mer chain in the dry state is $R_{dry} = N^{1/2}b$.

The above picture describes the swelling equilibrium well in the absence of ionic condensation. That is, if the average distance between two backbone charges on network chains is $l \geq l_B$, where $l \equiv L_0/Nf = b/f^{1/2} \approx 1.4b$ for our system. However, when the electrostatic interactions are stronger or equivalently $l < l_B$, the Onsager-Manning transition "condenses" a fraction of free counterions onto the chains and reduces the charge fraction of network chains to $\tilde{f} \approx b/l_B < f$ by neutralizing $Nf(1 - l/l_B)$ counterions.[25] As a result of the counterion condensation, fewer counterions contribute to the counterion-induced osmotic pressure, and the equilibrium swelling ratio decreases. Although eq 2 has no l_B dependence, it can still be used to gain insight on how strong electrostatic interactions (EI) deswell the gel in case of moderately charged gels.[15] One can tentatively replace the fraction of charges with the reduced charge fraction, $\tilde{f} \approx b/l_B < f$, in eq 2 and obtain a decreasing λ_0 with increasing l_B.

In the simulations, each hydrogel slab is highly swollen as schematically illustrated in Figure 1. Calculated values of equilibrium-swelling ratios λ_0 at $P = 0.0$ for each electrostatic strength l_B and polymerization degree N are given in Table 1. The data is well described by eq 2 ($\lambda_0 \sim N^{1/2}$). The data shown in Table 1 also reveals the decrease of equilibrium swelling ratio for increasing values of l_B: In our simulations, $l_B = 1b$ corresponds to a no-condensation regime ($l \geq l_B$ with $f = 0.5$ and $\nu = 3/5$), whereas at $l_B = 4b$ and $l_B = 8b$, counterions condense ($l < l_B$). The decrease of λ_0 with increasing l_B is also

DOI: 10.1021/acsmacrolett.5b00363
ACS Macro Lett. 2015, 4, 857−861

Table 1. Table of Equilibrium Swelling Ratios, λ_0, Thickness of Gap, δ_0, Excluded Volume (LJ), Coulombic Interaction Energies per Particle for the Simulated Hydrogel Systems at $D = D_0$[a]

N	l_B/b	λ_0	δ_0 [σ]	E^0_{LJ} [ϵ]	E^0_{Coul} [ϵ]
32	1	4.2(4)	72	0.1974(7)	0.1167(6)
32	4	3.5(9)	61	0.1487(4)	−0.7091(7)
32	8	1.9(2)	36	0.2104(3)	−2.4484(1)
128	1	7.4(0)	273	0.0328(9)	0.0718(1)
128	4	5.8(2)	214	0.0578(7)	−0.4466(7)

[a] $\lambda_0 \equiv L_0/R_{dry}$, where $R_{dry} = bN^{1/2}$ is size of a N-mer free chain in the dry state.

demonstrated by the simulation snapshots of fully equilibrated systems in Figure 2 for $N = 32$ PE gels. For clarity, we only show the monomers within a slice of thickness $\Delta y \approx 10b$.

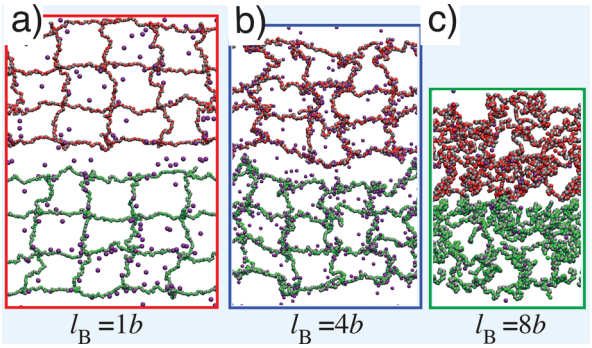

Figure 2. Snapshot taken from simulations of $N = 32$ double-gel systems of identical gels with various electrostatic coupling strengths l_B. The charge fraction is $f = 0.5$. Counterions are rendered in purple. $D/D_0 = 0.5$. For clarity, only monomers within a slice of thickness $\Delta y \approx 10b$ are shown. All snapshots are obtained via VMD.

Deformation: If the hydrogel PE gels are deformed uniaxially by decreasing the box height from D_0 to a prescribed height D, the previously discussed energy balance is altered. In an uncharged gel, a deformed gel reaches its equilibrium state by rearranging its monomers so that excluded-volume (or 3-body in a Θ-solvent) interactions balance the elastic energy of chains. In PE hydrogels, where the gel is highly swollen (i.e., $L_0 \sim N$; see eq 2 and Figure 1), the excluded-volume interactions are expected to be negligible. Hence, for intermediate deformations, hydrogels should balance their elastic and EI energies to reach mechanical equilibrium.

In PE hydrogel, upon deformation, EI energies can change in two ways compared to its stress-free (undeformed) state: (i) if the total gel volume decreases, the average distance between charged groups decreases. In turn, the EI energies become more negative. This is also the case if concentration of a simple electrolyte solution is increased. (ii) The distance between two adjacent backbone charges, l, decreases with deformation, and this triggers condensation or decondensation of counterions (a transition from $l > l_B$ to $l < l_B$[2]).

To see how the energetic balance changes with deformation, we calculated from simulation trajectories the absolute changes in the electrostatic, LJ pair interaction, and bond energies with respect to energy of the undeformed state, $\Delta E \equiv E(D) - E(D_0)$. The results are shown in Figure 3 as a function of compression ratio D/D_0. The LJ interaction energies (open symbols) weakly depend on the deformation ratios, regardless

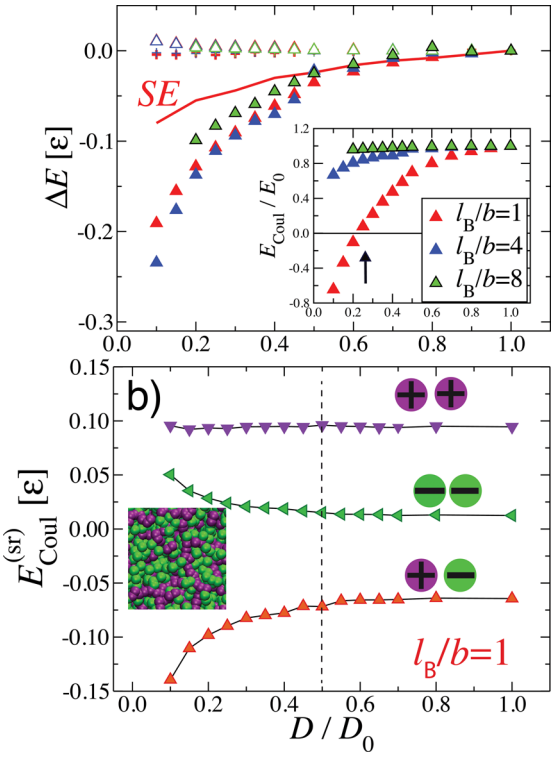

Figure 3. (a) Absolute change in the excluded volume (open symbols), Coulombic (filled symbols), bond (plus signs) energies for $N = 32$ hydrogels as a function of deformation ratio D/D_0 for various electrostatic interaction strengths, $l_B = 1b$, $4b$, $8b$. $\Delta E \equiv E(D) - E(D_0)$. Coulomb energies include both short-range and long-range interaction contributions. The solid red curve is the simulations results for a simple electrolyte (SE) with $l_B = 1b$. Insets show the relative changes for the Coulomb energies. (b) The counterion−counterion (− −), counterion−backbone (− +), and backbone−backbone (+ +) short-range Coulombic interaction energies for $l_B = 1b$. The arrow indicates the compression ratio at which the sign of EI energy changes.

of l_B. Similarly, the change in the bond energies (pluses) is almost negligible; the energy decrease in the (less stretched) chains parallel to the deformation axis cancels the energy increase of the (stretched) chains in the lateral directions.

In contrast to negligible changes in the LJ and bond energies, the electrostatic energies are altered significantly with deformation for all ionic strengths (Figure 3). As the volume of the hydrogels decreases, the average distance between the charged groups decreases. This in turn leads to an alteration in the Coulombic interactions, which are longer range than LJ interactions. For comparison, we also simulate a simple electrolyte (SE) solution at corresponding charge concentrations with $l_B = 1b$. The results are shown in Figure 3 with a red interpolation curve: The change in EI energies for the electrolyte solution is less than what we observe for PE gels with the same number of charged groups.

The effect of deformations on charge−charge interactions can be seen more clearly in Figure 3b, where we decompose the electrostatic short-range interaction energies between all charged groups: The counterion−counterion interaction energy (green left triangles in Figure 3b) increases. The energy between oppositely charged groups decreases (becomes more negative) since the charged backbone monomers and counterions start forming ionic structures such as dipoles.[26] Interestingly, overall repulsive interactions between the back-

DOI: 10.1021/acsmacrolett.5b00363
ACS Macro Lett. 2015, 4, 857−861

bone groups (down triangles) seem to be unchanged with deformation (Figure 3b), possibly for the same reason that gives no change in the bond energies.

For low ionic strengths ($l_B = 1b$), the sign of the total electrostatic energy changes from positive (repulsion dominated) to negative (attraction dominated) with deformation. Contrarily, in the system with $l_B = 4b$, $8b$, we find that the electrostatic energies are always negative regardless of hydrogel size. This is due to the fact that counterion condensation takes place even without deformations at high ionic strengths.

According to Figure 3, in terms of energy conversion, highly swollen gels with $l_B = 1b$, $4b$ are much more efficient compared to collapsed gels with $l_B = 8b$. This is more clear in the inset of Figure 3a, where we show the relative changes in the electrostatic energies. From the simulations of our defect-free gels, it turns out that the conversion efficiency depends on the stretchability of network chains: with deformation, to preserve its volume, ideally the gel would stretch the network chains in the unconstrained (lateral) directions. However, in the case of highly swollen gels (i.e., with $l_B = 1b$), the network chains are highly stretched even in the undeformed state. As a result, the gel volume decreases with decreasing D (red and blue symbols in Figure 4a). On the other hand, the gels with $l_B = 8b$ are

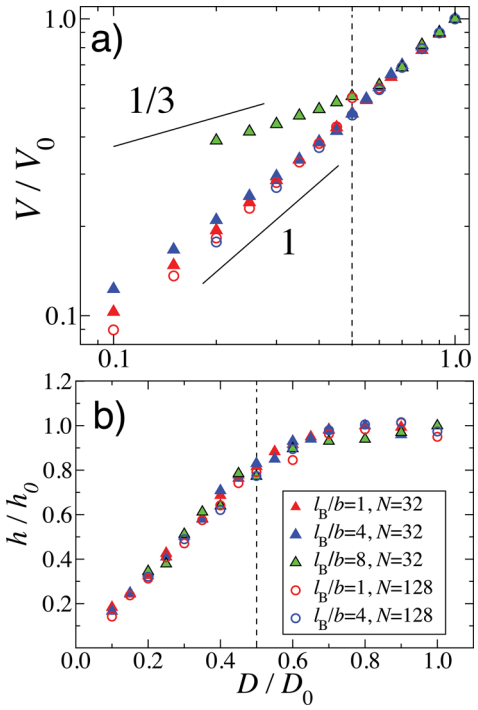

Figure 4. (a) Rescaled total volume of hydrogel systems as a function of rescaled box height for various PE gels in log–log scale. (b) Rescaled height of a single hydrogel slab (see Figure 1 for definitions). The dashed lines are $D/D_0 \approx 0.5$.

collapsed and the chains are loose (see the snapshot in Figure 2). Thus, upon deformation the gel can stretch its chains easier in the unconstrained directions, and the volume decrease with deformation is weaker for $l_B = 8b$ (green symbols in Figure 4a). This results in a smaller change in the counterion concentration in the gel, hence, a lower conversion efficiency.

The alterations in the EI energies observed in Figure 3, indeed, are a result of gel deformation. That is, for our setup, when $D/D_0 \leq 0.5$. For weak compressions (i.e., $D/D_0 \geq 0.5$), the decrease in the electrostatic energy is insignificant since the gel is not deformed (only the polymer-free gap deforms). This can be seen in Figure 4b, where we show the rescaled height of a single PE gel slab, h/h_0, as a function of compression ratio: the EI energies (Figure 3) begin to decrease significantly if $h/h_0 \leq 1$. Also note that in simulations the gap is visually detachable down to $D/D_0 \approx 0.2$.

Overall, our MD simulations suggest that PE hydrogels can be manipulated mechanically to store an excess electrostatic energy. The energetic change is more pronounced than that observed in a polymer-free simple electrolyte solution, as shown in Figure 3.

Our MD simulations with explicit counterions suggest that if a hydrogel undergoes strain-control deformations, an amount of mechanical energy applied is converted into electrostatic energy rather than elastic and excluded volume energies. The energetic change is due the decreasing translational entropy of counterion gas trapped inside the gel in combination with polymeric features of PE gels. This scenario is only possible if ionized counterions cannot vacate the gel, which is ensured by the electroneutrality condition inside the gel.

An energy converter or a sensor must change the form of energy into a usable or storable form after well-defined, successive thermodynamics cycles. Hydrogels are promising materials for soft electronic and actuator applications.[27] Here, indeed we show that a polyelectrolyte hydrogel's capability to preserve its overall electroneutrality gives rise to significant changes in the electrostatic energies upon compression. In low ionic-strength solvents, the energetic change is more dramatic. In gels that can undergo pH or redox-potential variations, the electrostatic-energy change observed in our MD simulations may induce pH or redox-potential changes inside the gels. One suggestion for a possible converter may be a PE hydrogel gel system in contact with one lower- and one higher redox-potential electrodes. By deforming the gel, the redox potential of the gel can be manipulated and the resulting potential difference can be harvested, analogously to a Carnot engine (i.e., heat baths are replaced by redox baths). In some systems, increasing ionic density in the gel structure may alter the local pH levels, which in turn can change the ionization degree of the charged groups on the hydrogel chains.[2,4]

AUTHOR INFORMATION

Corresponding Author

*E-mail: m-olvera@northwestern.edu.

Notes

The authors declare no competing financial interest.

ACKNOWLEDGMENTS

This work was supported by the Center for Bio-Inspired Energy Science (CBES), which is an Energy Frontier Research Center funded by the U.S. Department of Energy, Office of Science, Office of Basic Energy Sciences under Award Number DE-SC0000989. A.E. acknowledges Dr. Niels Boon and Dr. Edward Benigan for their careful readings of the manuscript and Dr. Jos Zwanikken for insightful discussions.

REFERENCES

(1) Lee, K. Y.; Mooney, D. J. *Chem. Rev.* **2001**, *101*, 1869–1880.
(2) Osada, Y.; Gong, J. P. *Adv. Mater.* **1998**, *10*, 827–837.
(3) Keplinger, C.; Sun, J.-Y.; Foo, C. C.; Rothemund, P.; Whitesides, G. M.; Suo, Z. *Science* **2013**, *341*, 984–987.

DOI: 10.1021/acsmacrolett.5b00363
ACS Macro Lett. 2015, 4, 857–861

(4) Sawahata, K.; Gong, J. P.; Osada, Y. *Macromol. Rapid Commun.* **1995**, *16*, 713−716.
(5) Dagdeviren, C.; et al. *Proc. Natl. Acad. Sci. U. S. A.* **2014**, *111*, 1927−1932.
(6) Kwon, H. J.; Osada, Y.; Gong, J. P. *Polym. J.* **2006**, *38*, 1211−1219.
(7) Yue, Y.; Kurokawa, T.; Haque, M. A.; Nakajima, T.; Nonoyama, T.; Li, X.; Kajiwara, I.; Gong, J. P. *Nat. Commun.* **2014**, *5*, 1−8.
(8) Peppas, N. A.; Hilt, J. Z.; Khademhosseini, A.; Langer, R. *Adv. Mater.* **2006**, *18*, 1345−1360.
(9) Liu, M.; Ishida, Y.; Ebina, Y.; Sasaki, T.; Hikima, T.; Takata, M.; Aida, T. *Nature* **2014**, *517*, 68−72.
(10) Johnson, B. D.; Beebe, D. J.; Crone, W. C. *Mater. Sci. Eng., C* **2004**, *24*, 575−581.
(11) Tanaka, T.; Nishio, I.; Sun, S.-T.; Ueno-Nishio, S. *Science* **1982**, *218*, 467−469.
(12) Donnan, E. A.; G, F. G. *Z. Phys. Chem.* **1932**, *162*, 346−360.
(13) Katchalsky, A.; Lifson, S.; Exsenberg, H. *J. Polym. Sci.* **1951**, *7*, 571−574.
(14) Mann, B. A.; Holm, C.; Kremer, K. *J. Chem. Phys.* **2005**, *122*, 154903.
(15) Mann, B. A.; Everaers, R.; Holm, C.; Kremer, K. *EPL (Europhysics Letters)* **2004**, *67*, 786−792.
(16) Yin, D.-W.; Olvera de la Cruz, M.; de Pablo, J. J. *J. Chem. Phys.* **2009**, *131*, 194907.
(17) Escobedo, F. A.; de Pablo, J. J. *Phys. Rep.* **1999**, *318*, 85−112.
(18) Yin, D.-W.; Yan, Q.; de Pablo, J. J. *J. Chem. Phys.* **2005**, *123*, 174909.
(19) Kremer, K.; Grest, G. S. *J. Chem. Phys.* **1990**, *92*, 5057.
(20) Grest, G. S.; Murat, M. *Macromolecules* **1993**, *26*, 3108−3117.
(21) Plimpton, S. J.; Pollock, R.; Stevens, M. Particle-Mesh Ewald and rRESPA for Parallel Molecular Dynamics Simulations in *Proc of the Eighth SIAM Conference on Parallel Processing for Scientific Computing* Minneapolis, MN; March, **1997**.
(22) Plimpton, S. *J. Comput. Phys.* **1995**, *117*, 1−19.
(23) Rubinstein, M.; Colby, R. H.; Dobrynin, A. V.; Joanny, J.-F. *Macromolecules* **1996**, *29*, 398−406.
(24) Panyukov, S. V. *Polym. Sci. U.S.S.R.* **1990**, *32*, 1247.
(25) Manning, G. S. *J. Chem. Phys.* **1969**, *51*, 924−933.
(26) Sing, C. E.; Zwanikken, J. W.; Olvera de la Cruz, M. *Macromolecules* **2013**, *46*, 5053−5065.
(27) Boon, N.; Olvera de la Cruz, M. *Soft Matter* **2015**, *11*, 4793.

DOI: 10.1021/acsmacrolett.5b00363
ACS Macro Lett. 2015, 4, 857−861